

Stationary and Dynamic Reference Frame Comparison Based Microgrid Application

ILYAS BENNIA^{1,2*}, YACINE DAILI^{1,2}, ABDELGHANI HARRAG^{1,2}, WALID ISSA³

¹Renewable Energy Deployment and Integration Team, Mechatronics Laboratory (LMETR), Optics and Precision Mechanics Institute, Ferhat Abbas University Setif 1, Setif, Algeria

²Electrotechnics Department, Faculty of Technology, Ferhat Abbas University Setif 1, Setif, Algeria

³Engineering & Maths Department, Sheffield Hallam University, Sheffield S1 1WB, UK

Abstract—This paper presents a brief comparison for voltage and current controllers implementation in both stationary and dynamic reference frame for a microgrid (MG) application. Diagrams of implementations are reviewed and the simulation results are presented to show the performance of each topology.

A. Keywords—microgrid; inner loops; voltage controller; current controller ; stationary reference; dynamic reference.

II. INTRODUCTION

Non-renewable resources, such as diesel, coal, and gas, are the primary energy sources of electrical energy produced by traditional power generators worldwide. However, the increasing demand for electricity, consumption of reserves of non-renewable resources, and generation of electrical energy from non-renewable resources conducted to environmental pollution. Therefore, the development of a distributed generation (DG) system using renewable resources such as solar and wind energy to produce electricity is necessary.

These renewable resources are difficult to integrate and exploit due to the stochastic behavior of their prime movers. A microgrid is an optimal solution to integrate and control distributed renewable resources and tied them to the utility grid. Using low-voltage distribution system consisting of DG units, energy storage devices, and load [1]. Additionally MG is able to operate in island or connected to a main distribution system, fig. 1 shows the general architecture of a MG[2]. In addition, compared with a single DG unit, a MG has high capacity and control flexibility to fulfill power-quality requirements [3].

Hierarchical control of MG was introduced in to deal with control challenges of MG and to endow smartness and flexibility to MGs [4], The hierarchical control based on three layers The primary layer include droop method [3] and virtual impedance loop [5], which are responsible for providing the voltage reference for inner loops which are often considered as level zero, inner loops are responsible for voltage and current regulating by a direct interaction with the VSIs, the secondary layer [6] allows the restoration of the deviations produced by the primary control and the tertiary layer manages the power flow between the MG and electrical distribution system [7].

The inner loops are responsible for voltage and current regulating by a direct interaction with the VSIs which are the

block stones and the significant components of a microgrid, inner loops consist of a cascaded control structure using a voltage and current controllers followed by a pulse-width-modulator (PWM). Here, the control loops regulate inverter state variables by computing an output voltage reference, which is the modulated signal by the PWM technic[8].

Inner loops can be implemented in a dq reference frame as described in [9]. using a conventional PI controller for a microgrid application although it can be implemented in $\alpha\beta$ stationary reference frame as studied in [10][11] using PR resonant controller which is adopted in many literature.

This paper is organized as follow. Primary control is illustrated in section two, Inner loops were reviewed in section three for either stationary and dynamic reference frame with a brief comparison to each other, simulation results in section four and the paper is concluded by section five.

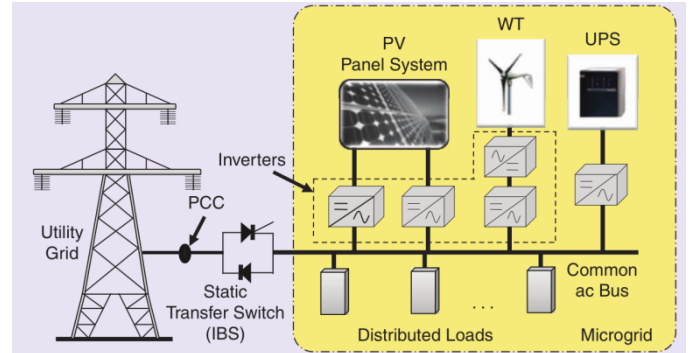


Figure 1. General architecture of a microgrid

III. PRIMARY CONTROL

Implemented locally primary control is responsible for power sharing, voltage and frequency regulation either in grid forming or grid following mode. This hierarchical layer sends control in intervals of several milliseconds to the VSIs to maintain the MG stability, communication in this control layer is undesired [12], the primary control is divided in two: inner loops responsible for regulating the power converters' voltage and current output, and the outer loop in charge of ensuring safe and correct power-sharing, inner loops have been widely studied in the literature however this topic still subject to research for enhancing the robustness against uncertainties[13], improving dynamic response, reducing unbalances and harmonic mitigation[14], developing control schemes plans

capable of operating in both grid and islanded modes and providing a smooth transition for MG operation modes. Outer loops are represented by the well-known droop control technique [15] and virtual impedance loop, droop control has the ability to adjust the frequency and the voltage amplitude of the voltage reference according to the active and reactive powers ensuring P and Q flow which is lead for power-sharing between VSIs, virtual impedance loop is added to improve the current sharing by fixing and normalizing the output impedance, figure (2) shows the primary control more details are mentioned in [16].

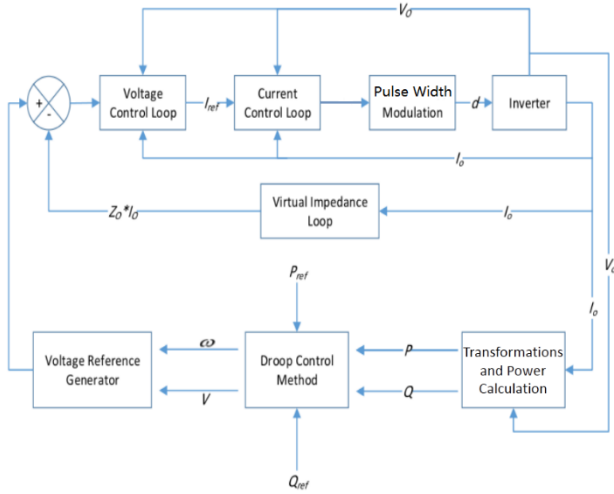


Figure 2. Primary control structure

IV. INNER LOOPS

The inner control loops are known as level -zero voltage and current loops, it consists of two controllers for ensuring the MG stability, the voltage controller received the voltage reference generated by the droop control and virtual impedance loop, which in turn generate the current reference for the current controller, this latter provides the voltage reference for the pulse width modulation bloc, In this section, inner loops controllers are reviewed in terms of the reference frame they are implemented[10].

A. Based $\alpha\beta$ on stationary reference frame

Stationary reference frame control, based on the abc/ $\alpha\beta$ transformation, a three-phase system can be represented in two independent single-phase systems. Generally the voltage and current controllers are based on a Proportional-resonant (PR) controller, where generalized integrators (GI) are used to perform zero steady-state error, transfer functions of voltage and current controllers expressed follow:

$$G_v(s) = K_{pv} + \frac{K_{iv}s}{s^2 + w_0} \quad (1)$$

$$G_i(s) = K_{pi} + \frac{K_{ii}s}{s^2 + w_0} \quad (2)$$

Where K_{pv} and K_{pi} are the proportional gains and K_{iv} , K_{ii} are the integral gains, and w_0 denotes resonant frequency. The

PR controller shows a high gain around the resonant frequency, which is tuned at the fundamental MG frequency[17]. As PR controller depends on the frequency, it should be carefully designed considering frequency response because even a small deviation of system frequency can reduce the advantage of its high gain around the resonant frequency. Thus, a frequency adaptive PR controller is proposed in [18], whose resonant frequency is estimated by a PLL instead of being fixed. In addition, harmonic compensator given in [10]by:

$$G_h(s) = \sum_h \frac{K_{th}s}{s^2 + (hw_0)^2} \quad (3)$$

Can be added in parallel with the PR controller for the fundamental grid frequency, where h is the order of the harmonic to be attenuated. This helps minimize the corresponding harmonic components in this paper harmonic compensators are not included. Figure (3) shows the block diagram of the inner control loops of a three-phase VSI in $\alpha\beta$ reference frame.

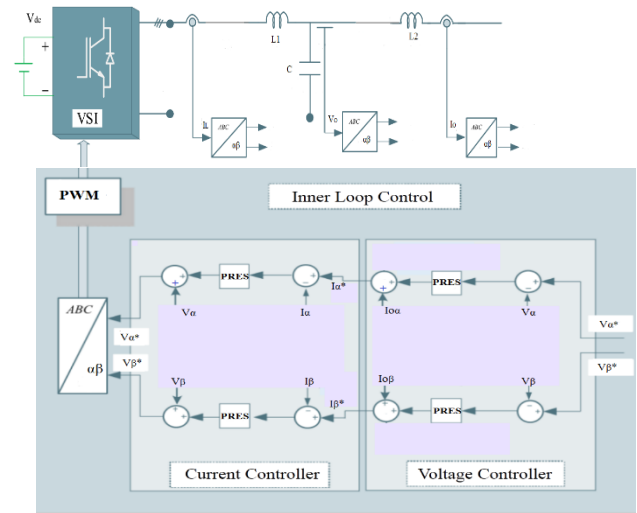


Figure 3. Voltage and current controllers in $\alpha\beta$ reference frame

Notice that the power calculation in $\alpha\beta$ frame using following equations:

$$p = v_\alpha \cdot i_{\alpha} + v_\beta \cdot i_{\beta} \quad (4)$$

$$q = v_\beta \cdot i_{\alpha} - v_\alpha \cdot i_{\beta} \quad (5)$$

B. Based on dq dynamic reference frame

Synchronous or dq reference frame, it converts grid voltage and current into a frame that rotates synchronously with the MG voltage vector by Park Transformation, three-phase time-varying signals are transformed into DC signals. In dq-control, PI controllers are typically used considering their capability of regulating direct signals without steady-state error[17]. The transfer's functions of a PI controllers are described follow:

$$G_{PI\text{voltage}}(s) = K_{pv} + \frac{K_{iv}}{s} \quad (6)$$

$$G_{PI\text{current}}(s) = K_{pi} + \frac{K_{ii}}{s} \quad (7)$$

Where K_{pv} and K_{pi} are referred to proportional gains and K_{vi} , K_{ii} are the integral gains, respectively. Established on symmetrical component theory, a voltage vector can be divided into positive-sequence component rotating anti-clockwise and negative-sequence component rotating clockwise. If a set of unbalanced signals is transformed into positive-sequence reference frame, the negative sequence component will be noted as AC signals oscillating at double the fundamental frequency same thing if positive-sequence components are transformed into negative-sequence reference frame. Because of this coupling between the two synchronous reference frames, PI controllers remain helpless to give satisfactory performance under unbalanced conditions[17]. This method requires two of PI regulators, one regulating only positive- sequence current in positive-sequence reference frame and the second controlling only negative-sequence current in negative-sequence reference frame, which allows the current in different sequences to be controlled within its own reference frame, notice that the capacity of harmonic compensation using PI controllers, is very low figure (4) shows the implementation of inner control loops in dq reference frame using PI controllers where Voltage feed forward and cross coupling is required , notice that the power calculation in dq frame as shown in the following equations:

$$p = v_d \cdot i_{od} + v_q \cdot i_{oq} \quad (8)$$

$$q = v_d \cdot i_{oq} - v_q \cdot i_{od} \quad (9)$$

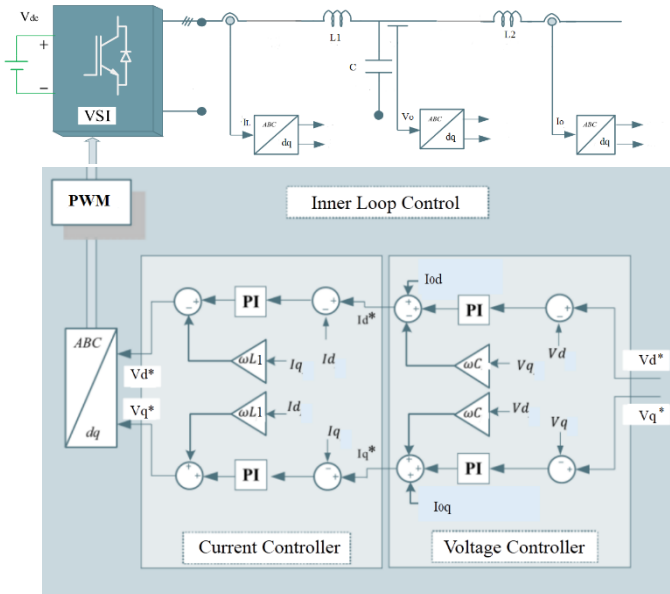


Figure 4. Voltage and current controllers in dq reference frame

V. SIMULATION RESULTS

In order to compare the performances of the voltage and current controllers under $\alpha\beta$ reference frame and dq reference frame a simulation was done using the control loops depicted in figure (3) for the $\alpha\beta$ reference frame and figure (4) for the dq reference frame both of them attached to a resistive load by MTLAB-Simulink software without including virtual impedance, the parameters are described in TABLE I.

Figure (5) and (10) show the tracking capabilities for both voltage controllers PR resonators in $\alpha\beta$ frame and PI in dq frame where they achieve a zero steady-state error with a negligible overshoot for the topology using PR resonant controller, same thing for current controllers in figure (6) and (11) where there is a high match between the reference current and the output current, voltage outputs are shown in figure (7) and figure (12) they present a fast dynamic and smooth response and reached the steady-state which confirms the effectiveness of the both regulators in the two reference frames. The measured active power in stationary reference frame reached the nominal power which is more accurate than the measured one in the dynamic reference frame notice that the technique of measurement is different in each topology as mentioned. Total harmonic distortion present in the stationary frame using PR regulator 1.19% is bigger than the amount of it in the dynamic reference using PI controllers 0.41%.

TABLE I. MICROGRID AND CONTROLLERS PARAMETERS

Parameter name	Acronym	Value	Units
Nominal AC voltage	V	220 rms	volt
Nominal frequency	f	50	Hertz
Load resistance	R	145.2	ohm
Filter output inductance	L1	0.003	H
Filter capacitance	C	4.8162e-06	F
Filter inductance	L2	0.001	H
Droop control parameters			
Proportional frequency droop	Kw	0.0003	W/rd
Proportional amplitude droop	Kv	0.004	Var/V
$\alpha\beta$ frame			
Proportional gain PRES voltage compensator	Kp v	0.2	A/V
Integral gain PRES voltage compensator	Ki v	100	A/(Vs)
Proportional PRES gain current compensator	Kp i	5	A ⁻¹
Integral gain PRES current compensator	Ki i	400	(As) ⁻¹
Cut-off frequency	W ₀	0.03 × ω _{nom}	rad/s
dq frame			
Proportional gain voltage compensator	Kp v	0.1	A/V
Integral gain voltage compensator	Ki v	3	A/(Vs)
Proportional gain current compensator	Kp i	20	A ⁻¹
Integral gain current compensator	Ki i	1000	(As) ⁻¹

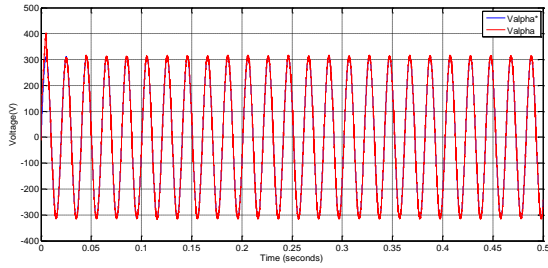


Figure 5. Valpha voltage tracking from voltage control loop

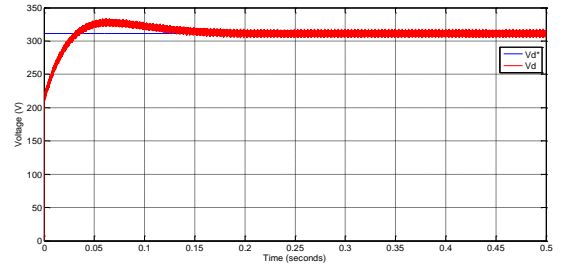


Figure 10. Vd voltage tracking from voltage control loop

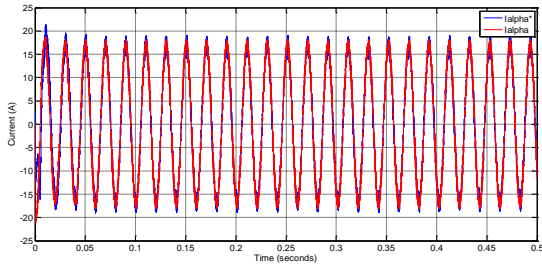


Figure 6. Ialpha current tracking from current control loop

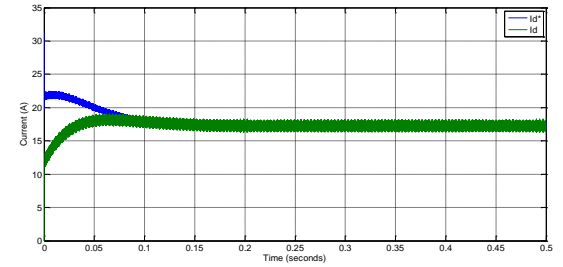


Figure 11. Id current tracking from current control loop

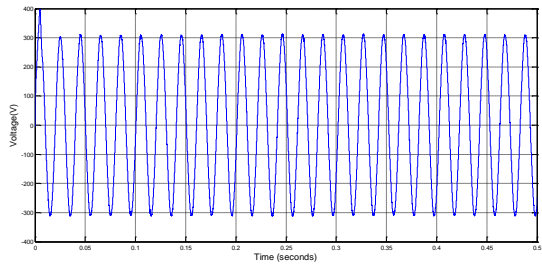


Figure 7. Output voltage phase A ($\alpha\beta$ framework)

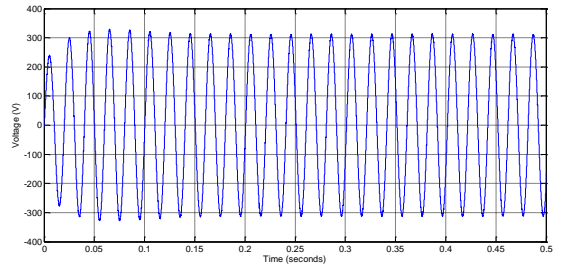


Figure 12. Output voltage phase A (dq framework)

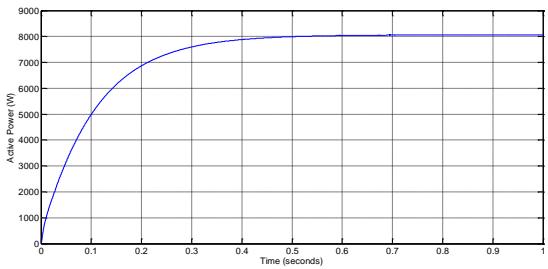


Figure 8. Active power curve ($\alpha\beta$ framework)

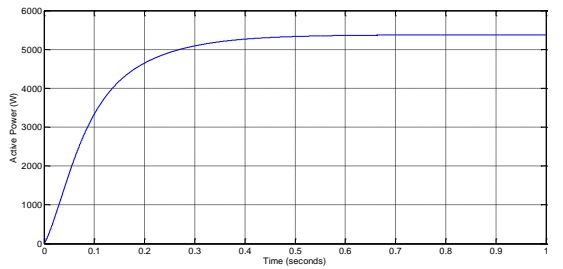


Figure 13. Active power curve (dq framework)

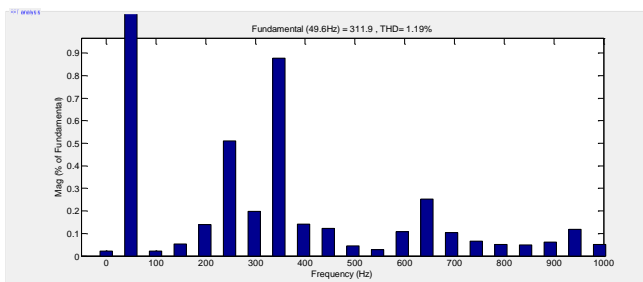


Figure 9. Spectrum frequency of output voltage in $\alpha\beta$ framework

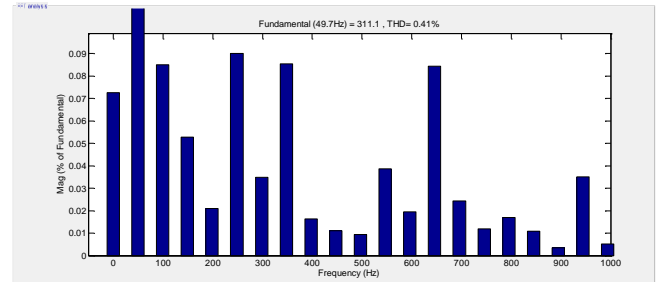


Figure 14. Spectrum frequency of output voltage in dq framework

VI. DISCUSSION AND CONCLUSION

In this paper we presented a brief comparison between the stationary and the dynamic reference frame for MG application, the primary control is described and the implementation of inner loops in both $\alpha\beta$ and dq frame is reviewed, as explained the structure implementation is simple with using of PR controllers when comparing the use of synchronous frame. There is no error in steady state condition when using either PR controllers or PI controllers, THD is more present when using PR controller, TABLE II shows a general comparison adopting many features.

TABLE II. GENERAL COMPARAISON OF USING STATIONARY AND DYNAMIC FRAMEWORK IN MICROGRIDS IMPLEMENTATION

Frames	$\alpha\beta$ frame	dq frame
Accuracy	Strong	High
Tracking	High	High
PI tuning	Difficult	Less difficult
Complexity	Medicum	High
THD	1.19%	0.41%

ACKNOWLEDGMENT

The Algerian Ministry of Higher Education and Scientific Research via the DGRSDT supported this research (PRFU Project code: A01L07UN190120180005).

REFERENCES

[1] M. A. Hossain, H. R. Pota, W. Issa, et M. J. Hossain, « Overview of AC microgrid controls with inverter-interfaced generations », *Energies*, vol. 10, n° 9, p. 1300, 2017.

[2] J. C. Vasquez, J. M. Guerrero, J. Miret, M. Castilla, et L. G. De Vicuna, « Hierarchical control of intelligent microgrids », *IEEE Ind. Electron. Mag.*, vol. 4, n° 4, p. 23-29, 2010.

[3] W. Issa, S. Sharkh, et M. Abusara, « A review of recent control techniques of drooped inverter-based AC microgrids », *Energy Sci. Eng.*

[4] I. Bennia, Y. Daili, et A. Harrag, « Hierarchical control of paralleled voltage source inverters in islanded single phase microgrids », présenté à Artificial Intelligence and Renewables Towards an Energy Transition 4, Springer, 2021, p. 302-313.

[5] W. Issa, M. Abusara, et S. Sharkh, « Impedance interaction between islanded parallel voltage source inverters and the distribution network », présenté à 7th IET International Conference on Power Electronics, Machines and Drives (PEMD 2014), IET, 2014, p. 1-6.

[6] I. Bennia, A. Harrag, Y. Daili, A. Bouzid, et J. M. Guerrero, « Decentralized secondary control for frequency regulation based on fuzzy logic control in islanded microgrid », *Indones J Electr Eng Comput Sci*, vol. 29, p. 85-100, 2023.

[7] R. Al Badwawi, W. R. Issa, T. K. Mallick, et M. Abusara, « Supervisory control for power

management of an islanded AC microgrid using a frequency signalling-based fuzzy logic controller », *IEEE Trans. Sustain. Energy*, vol. 10, n° 1, p. 94-104, 2018.

[8] T. Dragicevic, S. Vazquez, et P. Wheeler, « Advanced Control Methods for Power Converters in DG Systems and Microgrids », *IEEE Trans. Ind. Electron.*, 2020.

[9] I. Bennia *et al.*, « Design, Modeling, and Validation of Grid-Forming Inverters for Frequency Synchronization and Restoration », *Energies*, vol. 17, n° 1, p. 59, 2023.

[10] J. C. Vasquez, J. M. Guerrero, M. Savaghebi, J. Eloy-Garcia, et R. Teodorescu, « Modeling, analysis, and design of stationary-reference-frame droop-controlled parallel three-phase voltage source inverters », *IEEE Trans. Ind. Electron.*, vol. 60, n° 4, p. 1271-1280, 2012.

[11] Y. Han, P. Shen, X. Zhao, et J. M. Guerrero, « Control strategies for islanded microgrid using enhanced hierarchical control structure with multiple current-loop damping schemes », *IEEE Trans. Smart Grid*, vol. 8, n° 3, p. 1139-1153, 2015.

[12] D. Y. Yamashita, I. Vechiu, et J.-P. Gaubert, « A review of hierarchical control for building microgrids », *Renew. Sustain. Energy Rev.*, vol. 118, p. 109523, 2020.

[13] W. R. Issa, M. A. Abusara, et S. M. Sharkh, « Control of transient power during unintentional islanding of microgrids », *IEEE Trans. Power Electron.*, vol. 30, n° 8, p. 4573-4584, 2014.

[14] I. Bennia, Y. Daili, et A. Harrag, « LCL filter design for low voltage-source inverter », présenté à Artificial Intelligence and Heuristics for Smart Energy Efficiency in Smart Cities: Case Study: Tipasa, Algeria, Springer, 2022, p. 332-341.

[15] I. Bennia, A. Harrag, et Y. Dailia, « Small-signal modelling and stability analysis of island mode microgrid paralleled inverters », *J. Renew. Energ.*, vol. 24, n° 1, p. 105-120, 2021.

[16] B. Naji Alhasnawi, B. H. Jasim, A. Anvari-Moghaddam, et F. Blaabjerg, « A New Robust Control Strategy for Parallel Operated Inverters in Green Energy Applications », *Energies*, vol. 13, n° 13, p. 3480, 2020.

[17] J. Jia, G. Yang, A. H. Nielsen, et P. Rønne-Hansen, « Study of control strategies of power electronics during faults in microgrids », in *Hybrid-Renewable Energy Systems in Microgrids*, Elsevier, 2018, p. 109-146.

[18] I. Bennia, A. Harrag, et Y. Daili, « Adaptive Resonant Controller Based SOGI-FLL for Three-Phase Voltage Source Inverters », présenté à 2022 19th International Multi-Conference on Systems, Signals & Devices (SSD), IEEE, 2022, p. 756-762.